EPR investigation of iron-related centers in ^{57}Fe-doped $KTaO_3$

P. G. Baranov,* A. G. Badalyan, D. V. Azamat, V. A. Trepakov, A. P. Bundakova, E. A. Ruzanova, and V. S. Vikhnin
Ioffe Physico-Technical Institute, St. Petersburg 194021, Russia

H. Hesse and S. E. Kapphan
FB Physik, Universitaet Osnabrueck, 49069 Osnabrueck, Germany

(Received 2 November 2005; revised manuscript received 8 June 2006; published 24 August 2006)

Three dominant iron centers are studied in the as-grown ^{57}Fe-doped single $KTaO_3$ crystals. For each of the centers, which were labeled as rhombic Fe_{Ta}^{3+} and two axial Fe-related centers Fe_K^{3+}-O_I and $(Fe\frac{4}{2})$. The hyperfine structure due to an interaction with a single $I=\frac{1}{2}$ ^{57}Fe nucleus has been observed for the three centers and thus it was unambiguously shown that all three are iron related. The hyperfine interactions that were observed to be isotropic are 7.2×10^{-4} cm^{-1} for Fe_K^{3+}-O_I, 7.5×10^{-4} cm^{-1} for rhombic Fe_{Ta}^{3+}, and strongly anisotropic for $Fe\frac{4}{2}$: $A_{\parallel}=10.3\times10^{-4}$ cm^{-1} and $A_{\perp}=4.8\times10^{-4}$ cm^{-1}. The superhyperfine interactions with the next nearest-neighbor Ta ligands were observed for each center and these interactions were considered to be a measure of covalency effects. The covalency effect for irons in the Ta position is much larger compared to the K position and the hyperfine interaction constant for the Ta position is expected to be much larger compared to that for the K position. The large hyperfine interaction with Ta ligands which was observed for the $Fe\frac{4}{2}$ center strongly supports the Ta position for the iron and as a result it is suggested that the $Fe\frac{4}{2}$ center is a Fe^{5+} ion substituting for a Ta^{5+} and undergoing a strong axial crystal field. The axial symmetry seems to be caused by an off-center displacement of the small Fe^{5+} ion. It is suggested that the electronic configurations of the 5*d* shells of the Ta ligands repeat the electronic configuration of the 3*d* shell of the central transition-metal ion due to a cation-cation transfer of unpaired electrons from the central ion to the Ta ligand ion through the oxygen ligands.

DOI: 10.1103/PhysRevB.74.054111 PACS number(s): 77.84.Dy, 76.30.Fc, 76.70.Hb, 78.20.Ls

I. INTRODUCTION

The cubic perovskite $KTaO_3$ is an incipient ferroelectric having a cubic structure and does not undergo a ferroelectric phase transition down to lowest temperature. $KTaO_3$ is a useful host to study transition-metal impurities.[1,2] An introduction of transition-metal ions into ferroelectric oxides affect their optical, electrical, and magnetic properties. Fe ions were shown to exhibit the most varied behavior. There exist two possible impurity cation sites in a $KTaO_3$ perovskite lattice, the K^+ and Ta^{5+} sites. The K^+ ion is dodecahedrally coordinated by oxygen (12 nearest-neighbor oxygens along the ⟨110⟩ axes) and the Ta^{5+} ion is octahedrally coordinated by the oxygen (6 nearest-neighbor oxygen along the ⟨100⟩ axes). Electron paramagnetic resonance (EPR) is a method of choice for investigating the structure of transition-metal-related defects.[3,4] Observed hyperfine (HF) structure is a "fingerprint" for the chemical identity of the transition metal. But this approach could be very seldom applied to Ni or Fe impurities because of a very low abundance of isotopes having a nuclear magnetic moment. Iron has only one isotope, 2.15% abundant ^{57}Fe, with a small magnetic moment and nuclear spin $I=\frac{1}{2}$. Nickel has only one isotope, 1.13% abundant ^{63}Ni, with nuclear spin $I=\frac{3}{2}$. There is no chance to observe hyperfine structure from ^{57}Fe or ^{63}Ni nuclei in the crystals with natural abundances of Fe or Ni isotopes because the HF structure splitting is expected to be small compared to the EPR linewidth and the intensity of two ^{57}Fe hyperfine lines should be only 1% from the intensity of the central Fe. The intensity of four ^{63}Ni hyperfine lines should be only 0.25% of the intensity of the central Ni line. Thus one cannot differentiate between the Fe and Ni EPR spectra. In spite of this it was believed that EPR spectra of three dominant iron centers were identified in the as-grown nonenriched Fe-doped $KTaO_3$ crystals.[5–11] They were labeled as (i) rhombic Fe_{Ta}^{3+}, (ii) Fe_K^{3+}-O_I, and (iii) $Fe\frac{4}{2}$. The rhombic Fe_{Ta}^{3+} center has $S=\frac{5}{2}$ and is a Fe^{3+} at the Ta site. The Fe_K^{3+}-O_I or $Fe\frac{6}{2}$, is an axial center with Fe^{3+} at a K site in with two adjoining O vacancies, and in which the $S=\frac{5}{2}$ ion state experiences a strong axial crystal field resulting in an effective $S_{eff}=\frac{1}{2}$ ground state Kramers doublet with calculated[12] effective *g* components $g_{\parallel}^{e}=2$ and $g_{\perp}^{e}=3g_{\parallel}^{e}=6$. The iron-related center $Fe\frac{4}{2}$ center, originates from an $S=\frac{3}{2}$ state also experiencing a strong axial crystal field resulting in a Kramers $S_{eff}=\frac{1}{2}$ ground state with calculated[12] effective *g* components $g_{\parallel}^{e}=2$ and $g_{\perp}^{e}=2g_{\parallel}^{e}=4$.

It should be noted that the center $Fe\frac{4}{2}$ was not assigned to a specific ion and specific charge state, since no HF structure was observed and problems were encountered when comparing with published[6] $Fe\frac{4}{2}$ results. This EPR spectrum was observed for the first time[6] in $KTaO_3$ crystals strongly doped with Ni. However, some authors prefer the attribution to iron ions and *g* factors fit to an axial iron center with[13] $S=\frac{3}{2}$. Therefore $Fe^+(3d^3)$ at a K^+ site[14] or $Fe^{5+}(3d^7)$ at the Ta^{5+} site[15] have been discussed as possible sources of $Fe\frac{4}{2}$ EPR signals. To obtain information on the ^{57}Fe HF structure a $KTaO_3$ crystal was grown with 99% isotopically enriched ^{57}Fe and the result of such a study is presented in this paper.

II. EXPERIMENT

Several $KTaO_3$ crystals have been studied, which were iron doped by adding 0.5 mol % of naturally abundant Fe_2O_3

 ©2006 The American Physical Society

or 99% enriched $^{57}Fe_2O_3$ to the melt. The crystals were grown in air by the top-seed-solution-growth method at the University of Osnabrueck. EPR was performed using a JEOL CW spectrometer at the *X*-band frequency (9.3 GHz), equipped with a homemade evaporation cryostat for low-temperature measurements.

III. RESULTS

All the ^{57}Fe-doped as-grown $KTaO_3$ crystals show EPR spectra very similar to the patterns of the three dominant centers which were studied in the as-grown nonenriched $KTaO_3$:Fe, labeled as rhombic Fe_{Ta}^{3+}, Fe_K^{3+}-O_I, and $Fe\frac{4}{2}$. A general view of the EPR spectra in as-grown single $KTaO_3$:Fe (top) and $KTaO_3$:^{57}Fe (bottom) at 77 K is presented in Fig. 1. Fe_K^{3+}-O_I and $Fe\frac{4}{2}$ centers are marked for the one orientation $B\|[100]$. The other lines belong to the rhombic Fe_{Ta}^{3+} center. The difference in positions of EPR lines for rhombic Fe_{Ta}^{3+} centers in these two crystals are caused by a small deviation of the orientations. Generally, the HF interaction with the low abundant ^{57}Fe nucleus and superhyperfine (SHF) interaction with ligand nuclei are not visibly resolved and in this scale any difference between EPR spectra in $KTaO_3$ crystals doped with Fe in natural and isotope enriched form are barely be seen. Filled diamond, open diamond, and star marks the EPR lines of Fe_K^{3+}-O_I, rhombic Fe_{Ta}^{3+}, and $Fe\frac{4}{2}$ centers, respectively, which were investigated in an enhanced scale.

Figure 2 shows the EPR signal of three iron centers Fe_K^{3+}-O_I, rhombic Fe_{Ta}^{3+}, and $Fe\frac{4}{2}$ which were observed in the as-grown ^{57}Fe-doped $KTaO_3$ crystals for transitions which were marked by a filled diamond, open diamond, and star, respectively, in Fig. 1. For comparison each spectrum is presented on the same scale of the magnetic field. For all the spectra HF and SHF structure have been observed. The HF interactions with ^{57}Fe have, as will be shown later, mutually close magnitudes for all the spectra. In contrast, there is a big difference in SHF interaction values for Fe_K^{3+}-O_I centers on the one hand and rhombic Fe_{Ta}^{3+} and $Fe\frac{4}{2}$ on the other.

Figure 3 shows the lowest field transition of EPR spectra of a Fe_K^{3+}-O_I center in naturally abundant Fe-doped $KTaO_3$ (top) and ^{57}Fe enriched $KTaO_3$ (bottom). The spectrum is shown for $B\|[110]$. One of the three magnetically equivalent sites is oriented perpendicular to the field while the other two sites are oriented at $\theta=45°$ (not shown).

The simulated spectrum of $^{57}Fe_K^{3+}$-O_I (thin line in the bottom figure) calculated as a sum of two EPR spectra, presented in the middle part of the picture and observed in naturally abundant Fe-doped $KTaO_3$; one of which was shifted by 0.77 mT, i.e., equal to the HF structure constant with ^{57}Fe nuclei. Such a procedure could be done because for iron with natural abundance no HF splitting is observed, but for ^{57}Fe any EPR spectrum should be split in two patterns of equal intensity with a splitting that corresponds to the ^{57}Fe HF constant *A*. The thick line at the bottom part is the experimentally observed pattern.

Figure 4 shows one of the transitions of the EPR spectrum of the rhombic Fe_{Ta}^{3+} center in naturally abundant Fe-doped

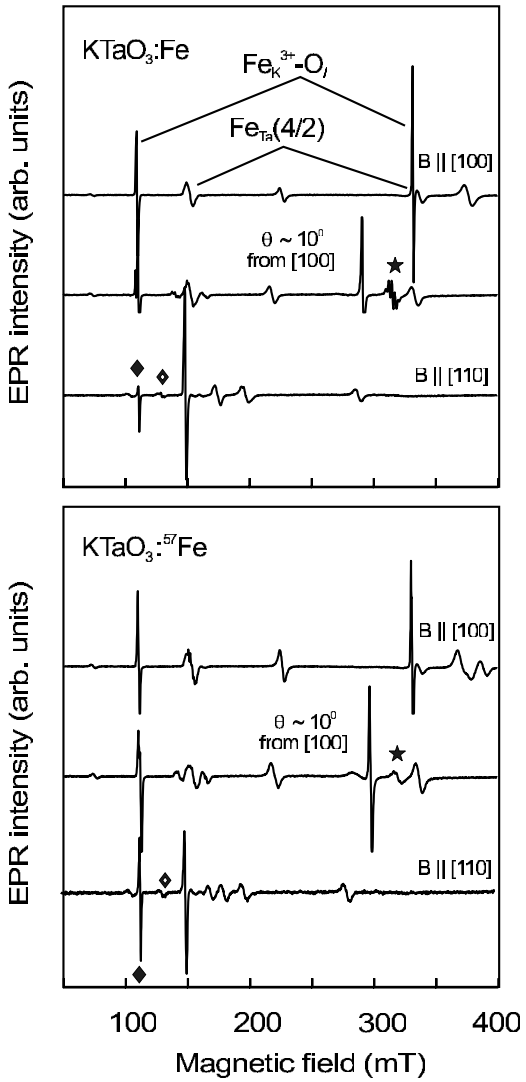

FIG. 1. A general view of the *X*-band EPR spectra in as-grown nonenriched single $KTaO_3$:Fe (top) and enriched $KTaO_3$:^{57}Fe (bottom) at 77 K at. Fe_K^{3+}-O_I and $Fe\frac{4}{2}$ centers are marked for one orientation $B\|[100]$, other lines belong to rhombic Fe_{Ta}^{3+} centers. Filled diamond, open diamond, and star marks the EPR lines of Fe_K^{3+}-O_I, $Fe\frac{4}{2}$, and rhombic Fe_{Ta}^{3+} centers, respectively. These spectra were investigated in enhanced scale.

$KTaO_3$ (top) and ^{57}Fe enriched $KTaO_3$ (two spectra at the bottom). The spectrum is shown for $B\|[110]$. The simulated spectrum (thin line in the middle) was prepared as a sum of two EPR spectra in naturally abundant Fe-doped $KTaO_3$ one of which was moved by 0.8 mT, i.e., equal to the HF structure constant with the ^{57}Fe nucleus. The amplitude of the magnetic field modulation was 0.5 and 0.2 mT for the well-resolved spectrum underneath.

Figure 5 shows the lowest field transition of the EPR spectra of $Fe\frac{4}{2}$ centers in naturally abundant Fe-doped $KTaO_3$ and ^{57}Fe enriched $KTaO_3$. The spectrum is shown for $\theta=10°$ from [100] (top) and $\theta=30°$ from [100] (bottom). For these magnetic field orientations HF splitting is distinctly observed. The simulated spectrum (thin line) was prepared as a sum of two EPR spectra in naturally abundant Fe-doped

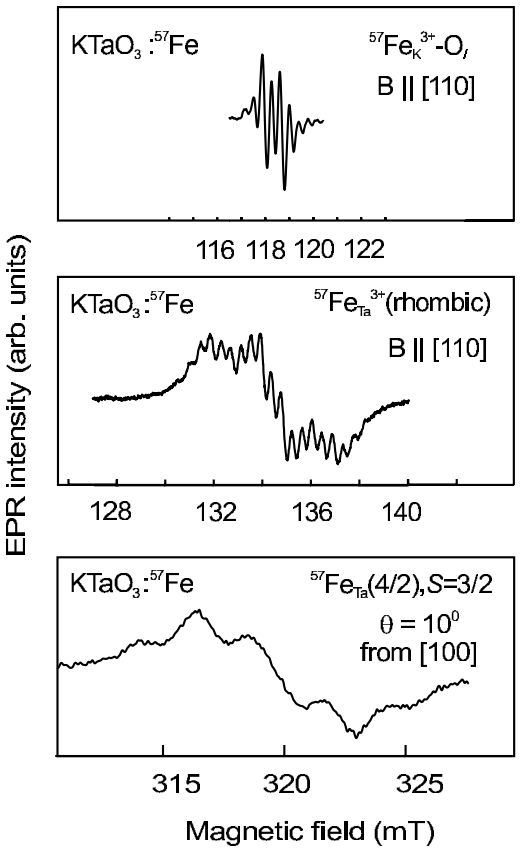

FIG. 2. *X*-band EPR spectra of three dominant iron centers which were identified in the as-grown ^{57}Fe-doped $KTaO_3$ crystals and labeled as $^{57}Fe_K^{3+}$-O_I, rhombic Fe_{Ta}^{3+}, and $^{57}Fe_{4/2}$. The magnetic field scale is the same for each spectrum.

$KTaO_3$ one of which was displaced by 1.05 and 0.8 mT for $\theta=10°$ and $\theta=30°$, respectively, i.e., equal to the HF structure splitting with ^{57}Fe nuclei for these orientations. The inset at the bottom shows the theoretical angle dependence of the HF splitting versus θ which corresponds to the experimental values for $\theta=10°$ and $\theta=30°$ (larger points in inset).

The spin Hamiltonian describing the EPR spectra has the standard form

$$\hat{H} = D\left[S_z^2 - \tfrac{1}{3}S(S+1)\right] + E(S_x^2 - S_y^2) + \mu_B \vec{B}\cdot\tilde{g}\cdot\vec{S} + \vec{S}\cdot\tilde{A}\cdot\vec{I} + \sum_{i=1}^{N}(\vec{S}\cdot\tilde{a}_i\cdot\vec{I}_i + \vec{I}_i\cdot\tilde{Q}_i\cdot\vec{I}_i), \quad (1)$$

where $S=\frac{5}{2}$ for the Fe^{3+} centers and $S=\frac{3}{2}$ for Fe_2^4 center. The first two terms correspond to the strong fine structure interaction (for axial centers $E=0$) that are experienced by Fe_K^{3+}-O_I and Fe_2^4, the third is the Zeeman interaction, the fourth, fifth, and sixth terms correspond to the hyperfine interaction with ^{57}Fe, and the superhyperfine and quadrupole interactions with the Ta nucleus, respectively; μ_B is the Bohr magneton; $\tilde{g}$ is the g tensor; $\tilde{A}$ is the HF interaction tensor, and $\tilde{a}_i$ and $\tilde{Q}$ are the tensors describing SHF and quadrupole interactions with the nucleus of the ith ligand ion. It should be noted that some higher order terms which describe the fine structure in cubic fields are omitted. The spin Hamiltonian parameters as $\tilde{g}$ tensor components, D and E for Fe-related centers can be found in Refs. 8 and 9. The HF and SHF structure parameters which were obtained for Fe-related centers in this paper are presented in Table I. $A_\parallel$ and $A_\perp$ are the values for B parallel to the axis of the center (one of $\langle 100\rangle$ directions) and B perpendicular to this axis, respectively. For iron centers the SHF splitting is presented only for some orientations. The SHF constant for Cu^{2+} centers was estimated for comparison with those for iron ions. For the two Ta ions located along the local z axis only $a_\parallel=0.3$ mT could be determined.

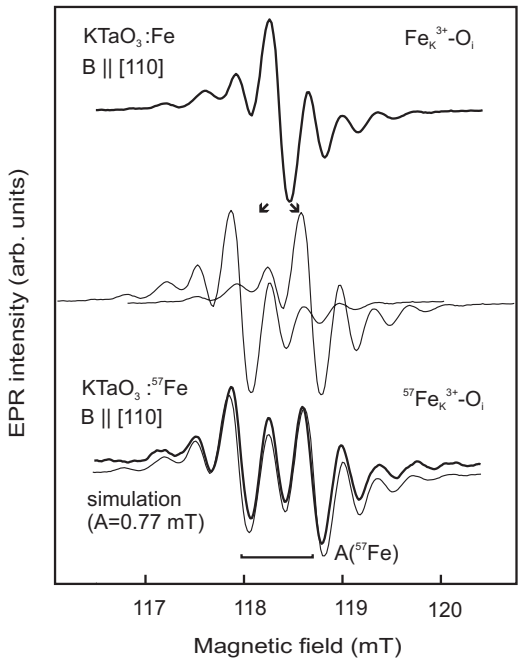

FIG. 3. The lowest field transition of *X*-band EPR spectra of Fe_K^{3+}-O_I center in naturally abundant Fe-doped $KTaO_3$ (top) and ^{57}Fe enriched $KTaO_3$ (bottom). The spectrum is shown for $B\|[110]$. The simulated spectrum (thin line in the bottom) was prepared as a sum of two EPR spectra (the middle part of the picture) in naturally abundant Fe-doped $KTaO_3$ one of which was moved by 0.77 mT, i.e., equal to hf structure constant with ^{57}Fe nuclei.

IV. DISCUSSION

Transition metals have a ground configuration which has no unpaired *s* electron. Nevertheless, an isotropic HF interaction is observed. The origin of the anomalous isotropic magnetic HF structure in the iron group is well understood qualitatively.[16] It is due to the existence of a finite spin density at the nucleus for which the method of core polarization provides reasonable agreement with experiment. The isotropic HF interaction for $3d$ elements is due to the polarization of $1s$, $2s$, and $3s$ shells by exchange with $3d$ electrons.

For the $^{57}Fe^{3+}$ centers almost isotropic HF interaction was observed, in contrast to the strong HF anisotropy which was observed for $^{57}Fe_2^4$ centers. There exists a problem of whether the Fe_2^4 center has a d^3 or d^7 configuration. The g

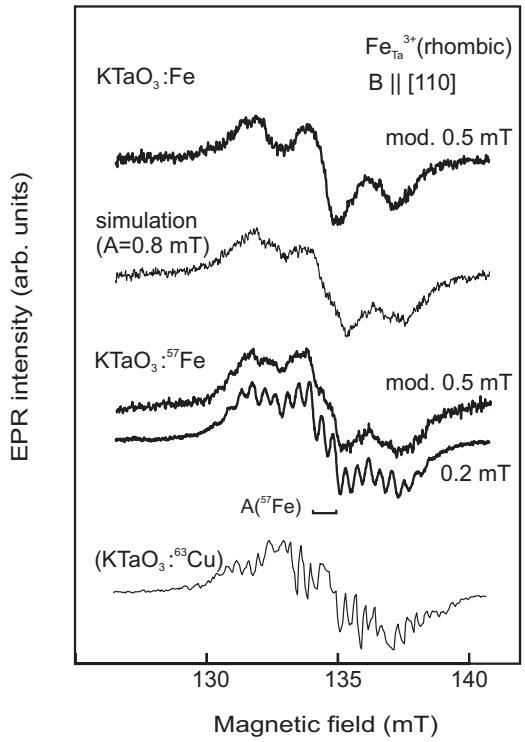

FIG. 4. One of the transitions of the *X*-band EPR spectra of rhombic Fe_{Ta}^{3+} center in naturally abundant Fe-doped $KTaO_3$ (top) and ^{57}Fe enriched $KTaO_3$ (two spectra at the bottom). The spectrum is shown for $B \| [110]$. The simulated spectrum (thin line in the middle) was prepared as a sum of two EPR spectra in naturally abundant Fe-doped $KTaO_3$ one of which was moved by 0.8 mT, i.e., equal to a hf structure constant with ^{57}Fe nuclei. For comparison the EPR signal of the $^{63}Cu^{2+}$ center in $KTaO_3$ is shown (the lowest pattern). The position of the line is shifted and the scale is normalized to the smallest splitting (0.4 mT) for rhombic Fe_{Ta}^{3+} center.

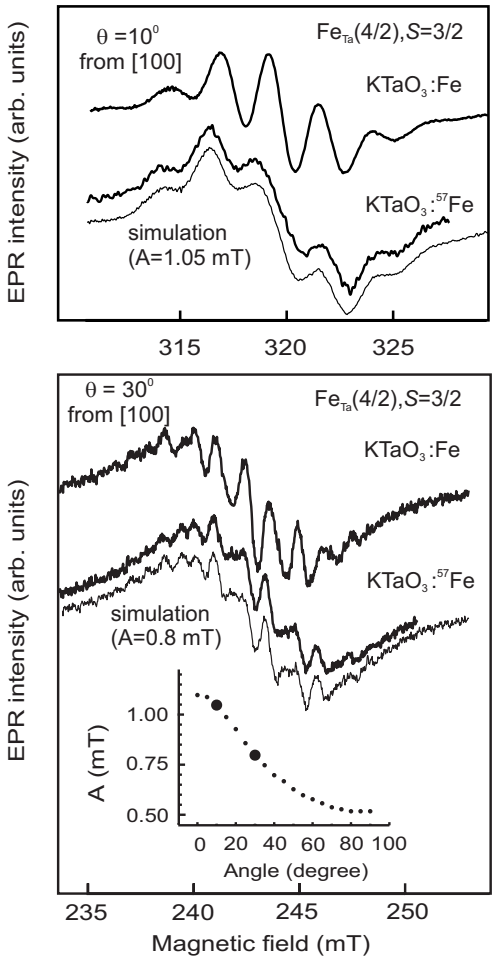

FIG. 5. The lowest field transition of *X*-band EPR spectra of the axial Fe-related center with spin $S=\frac{3}{2}$, or $Fe\frac{4}{2}$, in naturally abundant Fe-doped $KTaO_3$ and ^{57}Fe enriched $KTaO_3$. The spectrum is shown for the orientation of magnetic field $\theta=10°$ from [100] (top) and in the orientation of magnetic field $\theta=30°$ from [100] (bottom). The simulated spectrum (thin line) was prepared as a sum of two EPR spectra in naturally abundant Fe-doped $KTaO_3$, one of which was moved by 1.05 and 0.8 mT for $\theta=10°$ and $\theta=30°$, respectively, i.e., equal to the HF structure splitting with the ^{57}Fe nucleus. Inset at the bottom shows the theoretical angular dependence of HF splitting versus θ which corresponds to the experimental values for $\theta=10°$ and $\theta=30°$ (larger points in inset).

factor that was observed for the $Fe\frac{4}{2}$ center corresponds to the configuration with an orbital singlet in the ground state.[17] The ground state is an orbital singlet for a d^3 ion in an octahedral field (Fe^{5+} in Ta position, i.e., Fe_{Ta}^{5+}) with tetragonal distortion or for d^7 ion in K position. The HF structure observed for the $^{57}Fe\frac{4}{2}$ center (Table I) seems not to give unambiguous information about an electron configuration of this center.

What can really help to solve this problem is the observed SHF interaction with the Ta ligands. The important result is the large difference in SHF interactions with Ta for Fe_K^{3+}-O_I on the one hand, and rhombic Fe_{Ta}^{3+} and $Fe\frac{4}{2}$ on the other. Figure 2 demonstrates this difference. The splitting between the lines of SHF structure is 0.4 mT for the Fe_K^{3+}-O_I center and 2.4 mT for the $Fe\frac{4}{2}$. For rhombic Fe_{Ta}^{3+} centers two types of splitting were observed (Fig. 4): a strong splitting of about 2.2 mT and a weak splitting of about 0.4 mT. A similar SHF structure was observed for Cu_{Ta}^{2+} in $KTaO_3$ crystals.[5,18,19] That is why the pattern of one transition for Cu_{Ta}^{2+} is included at the bottom of Fig. 4. The real "weak" splitting for $Cu_{Ta}^{2+}(1)$ is 0.3 mT, but in Fig. 4, in order to compare qualitatively with the rhombic Fe_{Ta}^{3+} spectrum, this value was rescaled to 0.4 mT.

The big difference in SHF structure for Fe_K^{3+}-O_I on the one hand and rhombic Fe_{Ta}^{3+} and $Fe\frac{4}{2}$ on the other seems to be due to different positions of the Fe and as a result different covalency effects are expected. We believe that the total resolved SHF structure observed is due only to the interaction with the Ta^{5+} ions. The validity of this statement will be corroborated below. For the K position the covalency is very small. The opposite situation occurs for the Ta position where the covalency is strong. The SHF structure with Ta ligands is a probe for covalency effects. Thus for Fe in the K position the SHF interaction is small and for Fe in Ta position it is large. This conclusion shows that iron in $Fe\frac{4}{2}$ should occupy a Ta position and as a result only the d^3 configuration or Fe^{5+} charge state, will give an orbital singlet in the octahedral crystal field.[17] The anomalous intensity ratios of the

TABLE I. Parameters of the spin Hamiltonian for $^{57}Fe_K{}^{3+}$-O_I, rhombic $^{57}Fe_{Ta}{}^{3+}$, and $^{57}Fe_2^4$ centers. $A_\parallel$ and $A_\perp$ are the values for the magnetic field parallel to the local axis of the center (one of the ⟨100⟩ directions) and for magnetic field perpendicular to this axis, respectively.

Label	T (K)	HF constant $A(^{57}Fe)$ (10^{-4} cm^{-1})	SHF splitting $a(^{181}Ta)$ (mT)
$^{57}Fe_K{}^{3+}$-O_I	77	7.2	0.4 for $\theta=90°$
Rhombic $^{57}Fe_{Ta}{}^{3+}$	77	7.5	a(strong)=2.2 a(weak)=0.4 for $\theta=90°$
$^{57}Fe_2^4$	77	$A_\parallel=10.3$ $A_\perp=4.8$	$a=2.3$ for $\theta=10°$ $a=1.25$ for $\theta=30°$
$Cu_{Ta}{}^{2+}(1)$	300	$A_\parallel=173$ $A_\perp=30$	4 Ta in equatorial plane $a_\parallel=1.5$ $a_\perp=0.25$ 2 Ta in local z axis $a_\parallel=0.3$

SHF interaction components are apparently due to the existence of a strong quadrupole interaction (the tantalum nuclei are characterized by one of the largest known quadrupole moments). The existence of a strong quadrupole interaction with Ta ions comparable with the SHF interaction was shown by electron-nuclear double resonance[20] for Fe-related centers in $KTaO_3$.

Let us consider the SHF interaction, which is essential for obtaining information on the spin-density spatial distribution in the Fe-related and Cu-related centers. The observed SHF structure suggests the existence of several types of interactions with inequivalent ligand ions. If we exclude the interaction with impurities, $KTaO_3$ has ligand ions of three types, namely O^{2-}, K^+, and Ta^{5+}. The SHF interaction with oxygen may be disregarded, because only a very small fraction of the natural oxygen (0.038%) has a nonzero nuclear spin. In contrast to oxygen, the potassium and tantalum nuclei have a magnetic moment with nuclear spin I and a quadrupole moment Q_0 (in multiples of $|e|\times 10^{-24}$ cm^2): for ^{39}K (93.26%), $I=\frac{3}{2}$ and $Q_0=0.054$; and for ^{181}Ta (99.99%), $I=\frac{7}{2}$ and $Q_0=3.44$. The isotropic HF interaction constant for the $4s$ electron in the potassium atoms is 228 MHz. The corresponding constant for the tantalum $6s$ electron is 15 020 MHz and the anisotropic $5d$ electron HF interaction constant is[21] 445.4 MHz (without the angular coefficient). The isotropic and anisotropic HF interaction constants for the inner s and p electrons of the $K^+(3s,3p)$ and $Ta^{5+}(5s,5p)$ ions were theoretically calculated using the wave functions given in Ref. 22. It is essential to note that the constants for the tantalum exceed those for potassium by more than a factor of 50. Thus, even if the electron spin density is transferred equally to the potassium and tantalum nuclei—which, in actual fact, is not the case, because the spin-density transfer to the tantalum should be substantially larger due to both, the covalency effects and to the wave-function overlap—the SHF interaction constant with potassium should be negligible compared to that with the tantalum. Therefore, there are solid reasons for believing that the SHF structure observed in the experiments originates only from the interaction with the tantalum ions. It should be noted that in Ref. 23 EPR spectra of new axial centers have been identified in $KTaO_3$ which were assigned to Ta^{4+} and later reinterpreted[24] as O^- ions. Obviously, it cannot be Ta^{4+} because of a too small HF interaction with Ta, and, supporting the possible interpretation as O^- ions, we suggest that a F^+ center (oxygen vacancy with one unpaired electron) could be also considered as a model for the explanation of these EPR spectra.

There are at least two major mechanisms capable of contributing to the electron spin density at the tantalum nuclei: the overlap of the wave functions and the covalency.[25,26] The first one originates from the overlap of the wave functions related to the cluster under study, because the wave functions of different ions are, in general, not orthogonal to one another.[27] Covalency is a radically different effect in which an electron is transported between a magnetic ion and its diamagnetic environment. In the case of the $Cu^{2+}(3d^9)$ ions, an electron with the appropriate spin is transferred from the O^{2-} ion to the only empty orbital in the copper $3d$ shell to make the shell filled. In the case of the $Fe^+(3d^5)$ ions, electrons with the appropriate spin are transferred from the O^{2-} ion to the empty orbitals. One can invoke an additional mechanism of spin-density transfer to the tantalum nuclei. Such a mechanism could be a strong covalent transfer of oxygen electrons to the empty $6s$ and $5d$ shells of tantalum. In this case, the spin density at the oxygen—which is produced through the covalent transfer of one of the oxygen electrons to the copper or iron ion—is preserved in the covalent oxygen-electron transfer to the tantalum as well. Because the tantalum ions are located in the second coordination shell with respect to the iron or copper ions, the spin-density transport takes place primarily via the oxygen. This is a two-step process and hence, it is less efficient than the transfer to the oxygen. Nevertheless, the observed SHF interaction with the tantalum ions may provide indirect information on the spin density at the oxygen ions.

The effect of cation-cation transfer depends on an overlapping of oxygen wave functions with filled shells of Ta^{5+} and on a covalent transfer of oxygen wave functions into empty orbits of Ta^{5+}. These effects depend on the type of molecular orbit for MeO_6 complex (Me is a Fe or Cu ion). For the simplest $3d^9$ configuration only empty orbitals which could be created seem to be $\sqrt{3}(x^2-y^2)$ with some mixture of a $3z^2-r^2$ wave function for $5d$ electrons. In contrast, for d^3 and d^5 configurations the situation is more complicated because there are three and five unpaired electrons, respectively, on transition ion shells and we believe that a similar configuration will be repeated on the Ta ion due to the transfer of unpaired spins through the oxygen ligands. If this is true, the SHF structure of the Ta ions should be qualitatively similar to the HF structure for the central ion. This was really observed for the Cu^{2+} center in $KTaO_3$. The case of the Cu^{2+} center is the simplest for the iron group because only one unpaired electron interacts with the ligands. Thus it could be some model object to explain the SHF structure for more complicated cases: Fe^{3+} and Fe^{5+} centers.

Figure 6 presents the angular dependences of the EPR spectra observed in $KTaO_3$: ^{63}Cu crystals in the X band at

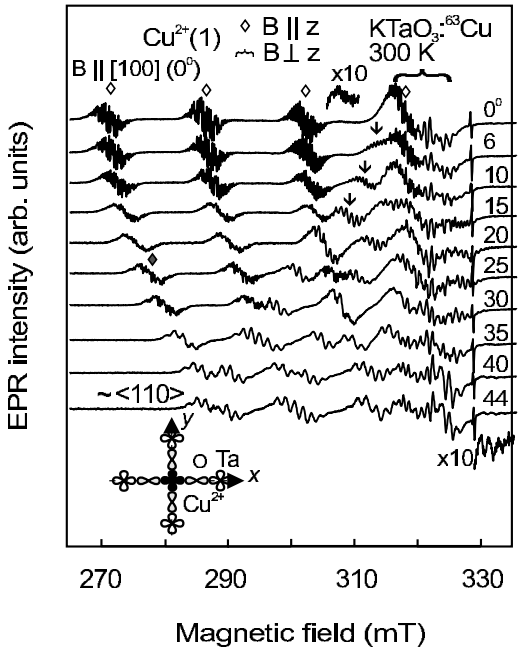

FIG. 6. Angular dependences of the *X*-band EPR spectra observed in $KTaO_3$: ^{63}Cu crystals at 300 K. The opened diamonds and brace specify the experimental positions of the EPR lines for single $Cu^{2+}(1)$ centers for $B\|z$ and $B\perp z$, respectively. The arrows show the positions of $Cu^{2+}(1)$ EPR lines for a small deviation from $B\perp z$, where the SHF structure is clearly observed. The high-gain spectrum ($\times 10$) shows two separate transitions for $Cu^{2+}(2)$, which are not overlapping with the $Cu^{2+}(1)$ spectrum. The filled diamond marks the EPR line that was placed in Fig. 4 for comparison with the EPR spectrum of Fe_{Ta}^{3+}. Schematic representation (bottom) of the central ion and ligand ion orbitals of symmetry e_g which are involved in σ bonding. For the central Cu ion and ligand Ta ions the $3d$ and $5d$ electrons are presented, respectively.

300 K. The crystal was rotated so that the ⟨100⟩ axis was perpendicular to the magnetic field. While there is a large number of EPR lines, practically all of them belong to two types of copper centers labeled by $Cu^{2+}(1)$ and $Cu^{2+}(2)$, which occupy the Ta position. The diamonds and brace specify the experimental positions of the EPR lines for single $Cu^{2+}(1)$ centers for $B\|z$ and $B\perp z$, respectively. In the $KTaO_3$ cubic crystal, the tetragonal axis of the Cu^{2+} centers may be aligned with any of the three equivalent ⟨100⟩ directions with equal probability and, therefore, the EPR spectrum taken in the $B\|\langle 100\rangle$ geometry exhibits the EPR lines corresponding to the magnetically inequivalent centers with $B\|z$, where z is the tetragonal symmetry axis of the center, and $B\perp z$ simultaneously. When the orientation deviates from $B\|\langle 100\rangle$, the signal corresponding to $B\perp z$ undergoes a further splitting. The arrows show the positions of $Cu^{2+}(1)$ EPR lines for small angle deviation from the orientation $B\perp z$, where SHF structure is clearly observed. The magnitude of this SHF interaction increases with the increasing of the deviation angle. It should be pointed out that the relative concentrations of the $Cu^{2+}(1)$ and $Cu^{2+}(2)$ centers depend on the sample and may vary over abroad range. For the sample in Fig. 6 the ratio of the intensities $Cu^{2+}(1)/Cu^{2+}(2)$ is about 10 which is why several lines belonging to the $Cu^{2+}(2)$ center and which do not overlap with the $Cu^{2+}(1)$ spectrum, are presented with an amplification of 10. Both centers were found within experimental error, to have a tetragonal symmetry. The EPR spectra obtained for each type of the Cu^{2+} centers in the $B\|z$ orientation consist of four relatively broad lines due to the HF interaction. Copper has two stable isotopes, ^{63}Cu (69.2%) and ^{65}Cu (30.8%); both isotopes have nuclear spins $I=\frac{3}{2}$ and nuclear g factors close in magnitude, and, therefore, for the ratio of the individual linewidths to the line separations observed experimentally in the EPR spectra, it is difficult to detect the copper isotopic splitting. To simplify the EPR spectra the enriched isotope ^{63}Cu was used. In some orientations, each copper HF component reveals an additional splitting caused by the SHF interaction with the ligands. The spectra could be described by a spin Hamiltonian (1) with $S=\frac{1}{2}$ and with omitting fine-structure terms and adding a quadrupole-interaction term for Cu. Due to quadrupole interactions the simple four lines spectrum was not observed for $B\perp z$ and the structure of the spectra is more complicated.

The EPR spectra observed for the $Cu^{2+}(1)$ centers have a resolved SHF structure, and two different kinds of SHF interactions which differ in the magnitude and character of the orientational dependences were observed.[19] The SHF structure with a small splitting, of the order of 0.3 mT for the orientations close to $B\|z$ (we call it a "weak" SHF interaction), was modulated in the magnetic field by a structure with a splitting of about 1.5 mT (accordingly, we call it a "strong" SHF interaction) that strongly decreases for the orientations close to $B\perp z$ (arrows in Fig. 6). What is more, a rotation of the magnetic field in the plane perpendicular to the z axis of the Cu^{2+} center does not seriously change this spectrum. That is why we can make the conclusion that no resolved SHF structure is observed for such orientation. The structure of the spectrum for $B\perp z$ is only due to HF and quadrupole interactions (that is the same order of magnitude as HF) with a Cu nucleus. For centers whose orientation was close to $B\|z$, a SHF structure with a splitting of 0.3 mT for $Cu^{2+}(1)$ was observed. When turned by more than 20° from this orientation, the lines broadened and the structure corresponding to the weak SHF interaction was practically unresolved. The structure due to the strong SHF interaction persisted and comprised at least seven lines with symmetrically distributed intensities. The total resolved SHF structure observed is due only to the interaction with the Ta^{5+} ions. More specifically, the weak interaction is due to the two Ta^{5+} ions located along the tetragonal axis of the center (the local z axis), while the strong interaction is associated with the four equivalent Ta^{5+} ions located in the equatorial plane perpendicular to the local z axis of the center. The anomalous intensity ratios of the strong SHF interaction components are due to the existence of a strong quadrupole interaction.

Because $g_\| > g_\perp = 2$, the wave function of the Cu^{2+} ion has the form $3d_{x^2-y^2}$, where the local symmetry axis z is directed along ⟨100⟩ (Fig. 6). As soon as the strong SHF interaction with Ta ligands of the Cu^{2+} centers decreases with an increasing of the angle between B and the z axis, (Fig. 6), and the SHF structure does not depend on the orientation of B in the plane perpendicular to the z axis we can conclude that the

symmetry of the wave function of unpaired electron on the Ta ligand in the plane perpendicular to the z axis is the same as for Cu^{2+} that is $5d_{x^2-y^2}$. Indeed, the angle dependences for HF interactions with Cu and SHF interactions with four equatorial Ta ligands is qualitatively the same: strong for $B\|z$ and almost six times smaller for $B\perp z$. The wave function of an unpaired electron for the Cu^{2+} center is presented in the bottom of Fig. 6. The z axis is perpendicular to the figure plane. The reproducing of the electronic wave function of central ion on the Ta ligands is observed.

For the Fe_2^4 center strong covalency effects seem to be in contradiction with the Fe^+ in the K position. What is more, Fe^+ (like Mn^+ or Mn^0) is a not natural charge state for as-grown crystals. For instance, such charge states were never observed in as-grown alkali halide crystals and could be produced only by optical excitation or x irradiation (see, e.g., Refs. 28 and 29). Thus, we prefer the attribution of the spectra to Fe^{5+} in the Ta position because it is very natural state. Such behavior was observed for $3d^3$ ions in $SrTiO_3$.[30] The axial symmetry seems to be due to an off-center position of the Fe^{5+} in the Ta^{5+} site because no charge compensation is needed. Such an impurity ion is a good example for the possibility of an off-center behavior.[31] An off-center position seems to be a direct consequence of the small enough ionic radius of the Fe^{5+} ion with respect to the host lattice Ta^{5+} which it replaced. Here the Fe^{5+}-O^{2-} ion displacements toward each other may lead to a total energy lowering due to a covalency increase. Using similarities of the orientation dependences of the HF and the SHF splitting for Fe^{5+} it was suggested that the electronic configurations of the $5d$ shell of the closest Ta ion located on the local z axis of the Fe_2^4 center can repeat the electronic configuration of the central ion. The complicated form of the SHF structure with a single Ta nucleus could be due to a strong quadrupole interaction for Ta, which could be comparable in magnitude to the SHF splitting. It should be noted that the model Fe^{5+}-V_0 (Ref. 15) can also not be totally excluded. In all these cases pair centers such as Cu-Cu pairs[18,19] are excluded from consideration because only a two-line HF splitting has been observed characteristic for ^{57}Fe (Figs. 3–5).

V. SUMMARY

Three dominant iron centers are studied in the as-grown isotopically enriched ^{57}Fe-doped single $KTaO_3$ crystals. For each of the centers, labeled as $Fe_K^{3+}-O_I$, rhombic Fe_{Ta}^{3+}, and Fe_2^4 centers, a two-line HF structure due to interaction with one ^{57}Fe nuclei has been observed. Thus it has been unambiguously shown that all these centers are iron related. The HF interaction was observed to be isotropic for Fe^{3+} centers and strongly anisotropic for Fe_2^4. The SHF interactions with the next nearest-neighbor Ta ligands were observed for each center and these interactions were considered to be a measure of covalency effects. The covalency effect for the Ta position of iron is much larger when compared to the K position and as a result the SHF interaction value for the Ta position is much larger compared to that for Fe in the K position. The large HF interaction with Ta ligands which was observed for the Fe_2^4 center strongly supports both the Ta position of iron in this case and the suggestion that it is a Fe^{5+} ion which substitutes for Ta (Fe_{Ta}^{5+}). The axial symmetry seems to be caused by the off-center position of Fe^{5+} ion in a Ta site. It was suggested that the electronic configurations of the $5d$ shells of the Ta ligands repeat the electronic configuration of the $3d$ shell of the central transition-metal ion due to a cation-cation transfer of unpaired electrons from the central ion to the Ta ligand ion through the oxygen ligands.

ACKNOWLEDGMENTS

This work was supported by NATO under Grant No. LG980375, AVCR No. KJB1010301, RFBR under Grants No. 04-02-17632 and No. 05-02-17817 and Programs of RAS "Spintronics," P-03 "Quantum Macrophysics," and "Quantum Nanostructures."

*Electronic address: pavel.baranov@mail.ioffe.ru

[1] K. A. Müller, J. Phys. (France) **42**, 551 (1981).
[2] B. E. Vugmeister and M. D. Glinchuk, Rev. Mod. Phys. **62**, 993 (1990).
[3] A. Abragam and B. Bleaney, *1970 Electron Paramagnetic Resonance of Transition Ions* (Oxford University Press, Oxford, 1970).
[4] Miguel Moreno, J. Phys. Chem. Solids **51**, 835 (1990).
[5] D. M. Hannon, Phys. Rev. **164**, 366 (1967).
[6] M. M. Abraham, L. A. Boatner, D. N. Olson, and U. T. Hoechli, J. Chem. Phys. **81**, 2528 (1984).
[7] I. P. Bykov, M. D. Glinchuk, A. A. Karmazin, and V. V. Laguta, Fiz. Tverd. Tela (Leningrad) **25**, 1239 (1983) [Sov. Phys. Solid State **25**, 2153 (1983)].
[8] H.-J. Reyher, B. Faust, M. Maiwald, and H. Hesse, Appl. Phys. B **63**, 331 (1996).
[9] H.-J. Reyher, B. Faust, M. Kading, H. Hesse, E. Ruza, and M. Wohlecke, Phys. Rev. B **51**, 6707 (1995).
[10] B. Faust, H.-J. Reyher, and O. F. Schirmer, Solid State Commun. **98**, 445 (1996).
[11] H.-J. Reyher, N. Hausfeld, and M. Pápe, J. Phys.: Condens. Matter **12**, 10599 (2000)
[12] E. S. Kirkpatrick, K. A. Müller, and R. S. Rubins, Phys. Rev. **135**, A86 (1964).
[13] A. P. Pechenyi, M. D. Glinchuk, T. V. Antimirova, and W. Kleeman, Phys. Status Solidi B **168**, K27 (1991).
[14] V. V. Laguta, M. D. Glinchuk, I. P. Bykov, J. Rosa, L. Jastrabik, R. S. Klein, and G. E. Kugel, Phys. Rev. B **52**, 7102 (1995).
[15] V. E. Bursian, V. S. Vikhnin, L. S. Sochava, S. Kapphan, and H. Hesse, Phys. Solid State **39**, 547 (1997); D. V. Azamat, S. A. Basun, V. E. Bursian, A. G. Razdobarin, L. S. Sochava, H. Hesse, and S. Kapphan, *ibid.* **41**, 1303 (1999).
[16] A. Abragam and B. Bleaney, *1970 Electron Paramagnetic of Transition Ions* (Ref. 3), p. 702.

[17] A. Abragam and B. Bleaney, *1970 Electron Paramagnetic of Transition Ions* (Ref. 3), p. 365.
[18] D. V. Azamat, A. G. Badalyan, P. G. Baranov, P. P. Syrnikov, V. A. Trepakov, J. Rosa, and L. Jastrabik, JETP Lett. **69**, 943 (1999).
[19] P. G. Baranov, A. G. Badalyan, and D. V. Azamat, Phys. Solid State **43**, 98 (2001).
[20] M. D. Glinchuk, Izv. Akad. Nauk SSSR, Ser. Fiz. **51**, 2124 (1987), and references therein; V. V. Laguta, A. A. Karmazin, I. P. Bykov, V. G. Grachev, and V. V. Troitckii, *ibid.* **51**, 2130 (1987).
[21] J. R. Morton and K. F. Preston, J. Magn. Reson. (1969-1992) **30**, 577 (1978).
[22] E. Clementi and C. Roetti, At. Data Nucl. Data Tables **14**, 177 (1974); A.D. McLean and R. S. McLean, *ibid.* **26**, 197 (1981).
[23] V. V. Laguta, M. I. Zaritskii, M. D. Glinchuk, I. P. Bykov, J. Rosa, and L. Jastrabik, Phys. Rev. B **58**, 156 (1998).
[24] M. Maiwald and O. F. Schirmer, Europhys. Lett. **64**, 776 (2003).
[25] E. Simanek and Z. Sroubek, *in Electron Paramagnetic Resonance*, edited by S. Geschwind (Plenum, New York, 1972), p. 535.
[26] O. F. Schirmer, J. Phys. C **6**, 300 (1973).
[27] B. S. Gourary and F. J. Adrian, Phys. Rev. **105**, 1180 (1957).
[28] R. A. Zhitnikov, P. G. Baranov, N. I. Melynikov, and N. G. Romanov, Sov. Phys. Solid State **12**, 2469 (1971) [Fiz. Tverd. Tela (S.-Peterburg) **12**, 3052 (1970)].
[29] H. Vrielinck, F. Callens, P. Matthys, S. V. Nistor, D. Ghica, and D. Schoemaker, Phys. Rev. B **64**, 024405 (2001).
[30] K. A. Müller, Th. von Waldkirch, W. Berlinger, and B. W. Faughnan, Solid State Commun. **9**, 1097 (1971).
[31] K. A. Müller W. Berlinger, and J. Albers, Phys. Rev. B **32**, 5837 (1985).